

## Mechanisms of the plasma rotation effect on the type-I ELM in tokamaks

N. Aiba 1), M. Furukawa 2), M. Hirota 1), N. Oyama 1), A. Kojima 1), S. Tokuda 3) and M. Yagi 1)

1) Japan Atomic Energy Agency, Naka, Ibaraki 311-0193, Japan

2) Graduate School of Frontier Science, University of Tokyo, Kashiwa, Chiba 277-8561, Japan

3) Research Organization for Information Science and Technology, Tokai 319-1106, Japan

e-mail contact of main author: aiba.nobuyuki@jaea.go.jp

**Abstract.** A toroidal rotation effect on a type-I ELM is investigated numerically in JT-60U H-mode plasmas. This analysis shows that a sheared toroidal rotation can destabilize a type-I ELM, and has an impact on the achievable pressure gradient and the type-I ELM behavior in JT-60U. To investigate this destabilizing mechanism, energies that are distinguished by physics are introduced. By comparing them, it is found that an edge localized MHD mode is destabilized by the difference between an eigenmode frequency and an equilibrium toroidal rotation frequency, which becomes more effective in the shorter wavelength region. Based on this result, an effect of a poloidal rotation is also investigated. Under the assumption that a change of an equilibrium by a poloidal rotation is negligible, it is identified numerically that a poloidal rotation can have both a stabilizing effect and a destabilizing effect on the edge MHD stability according to the direction of the poloidal rotation.

### 1. Introduction

An ideal magnetohydrodynamic (MHD) mode unstable near the plasma surface is thought as a cause of a type-I edge-localized mode (ELM), which constrains the maximum pressure gradient and its width at tokamak edge pedestal [1]. Since the type-I ELM induces a large heat load on a divertor and a wall, it should be suppressed or its amplitude needs to be reduced.

Recent experimental results in JT-60U show that a toroidal rotation near pedestal has an impact on the ELM behavior [2, 3]. For example, an ELM frequency increases by changing the direction of a toroidal rotation, and as the result, the type of ELM changes from the type-I ELM to the grassy ELM [2]. Therefore, it is important to understand a toroidal rotation effect on the edge MHD stability, which drives not only the type-I ELM but also the grassy-ELM whose mode structure is narrower than that of the type-I ELM [4, 5].

Previous works reported that an edge localized MHD mode, called a peeling-ballooning mode, can be destabilized by a toroidal rotation with shear [6, 7]. In particular, Ref. [7] investigated a toroidal rotation effect on the stability boundary of edge localized MHD modes, and identified that this effect limits an achievable pressure gradient due to the destabilization of finite- $n$  edge MHD modes even though a ballooning mode stability is scarcely changed. Here  $n$  is the toroidal mode number. However, the mechanism of this destabilization is still unclear. In addition, recently, not only a toroidal rotation but also a poloidal rotation are observed near edge pedestal at high spatial- and fast time-resolutions [8, 9], so that it should be necessary to identify whether a poloidal rotation also affects the edge MHD stability or not.

In this paper, we focus on the rotation effects on the MHD stability, and discuss an impact of the effect on ELM behavior. At first, the stability of the edge-localized MHD mode in JT-60U ELMy H-mode plasmas is studied numerically with an effect of a toroidal rotation, and the importance of this effect on the observed ELM behavior is evaluated. Next, we introduce new definitions of energy that are distinguished by physics for investigating mechanisms that a toroidal rotation with shear destabilizes an edge localized MHD mode. After that, an effect of a poloidal rotation on the edge MHD stability is investigated, and is compared with that of a toroidal rotation.

This paper is organized as follows. Section 2 shows the numerical results of the stability analysis with/without a toroidal rotation effect in JT-60U plasmas, and discusses the impact of this effect on the type-I ELM in JT-60U. Section 3 discusses mechanisms that a toroidal rotation with shear destabilizes an edge localized MHD mode. Section 4 investigates an effect of a poloidal rotation on the edge MHD stability. Section 5 presents a summary of this work.

## 2. Toroidal rotation effect on the edge MHD stability in JT-60U ELMY H-mode plasmas

In this section, we investigate an effect of a toroidal rotation on the type-I ELM in JT-60U numerically. The equilibria analyzed here are obtained by the reconstruction with the experimental data of E49228 and E49229 plasmas in JT-60U; the details of these plasmas are shown in Ref. [10]. As discussed in this reference, these plasmas have the same toroidal magnetic field at the axis  $B_0 = 4.0[\text{T}]$  and the plasma current  $I_p = 1.6[\text{MA}]$ , but the plasma rotation profiles are different between E49228 and E49229, whose toroidal rotation are in the co-(CO.) and ctr-(CTR.) directions to the plasma current, respectively. Such a difference of the rotation profiles are realized by adjusting the momentum input with neutral beam injection (NBI). By changing the rotation profile from CO. to CTR., the type-I ELM frequency increases from  $\sim 37[\text{Hz}]$  to  $\sim 45[\text{Hz}]$ , and the ELM energy loss becomes about half from  $\sim 89[\text{kJ}]$  to  $\sim 46[\text{kJ}]$ .

Figure 1 shows the profiles of (a) the temperatures of ion  $T_i$  and electron  $T_e$ , (b) the electron number density  $n_e$  and the pressure  $p$ , (c) the toroidal rotation frequency  $\Omega_t$ , and (d) the parallel current density  $\langle \mathbf{j} \cdot \mathbf{B} \rangle / \langle B^2 \rangle$  and the safety factor  $q$ , respectively; these indicate the profiles just before the ELM crash. Here  $\rho_{vol.}$  is the radial coordinate defined as  $\rho_{vol.} \equiv \sqrt{V(\psi)/V_{tot.}}$ ,  $V$  is the volume in each flux surface,  $\psi$  is the poloidal flux normalized as  $\psi = 0 (= 1)$  at the axis (surface),  $V_{tot.}$  is the plasma total volume,  $\mathbf{j}$  is the plasma current density,  $\mathbf{B}$  is the magnetic field, and bracket  $\langle f \rangle$  means the flux averaged value of  $f$ . The  $\langle \mathbf{j} \cdot \mathbf{B} \rangle / \langle B^2 \rangle$  profile is obtained by estimating a bootstrap current, a neutral beam driven current, and an ohmic current with the ACCOME code [11]. The effective charge  $Z_{eff}$  and the poloidal beta  $\beta_p$  are (2.6, 0.85) and (2.8, 0.81) in the E49228 (CO.) and the E49229 (CTR.) plasmas, respectively. Hereafter, the E49228 and the E49229 plasmas are called as CO. and CTR. plasmas. Note that the  $T_i$  profiles outside the top of the  $T_i$  pedestal ( $\rho_{vol.} > 0.93$ ) are similar to each other but the  $n_e$  profile of the CTR. plasma is different from that of the CO. plasma; the  $n_e$  pedestal top and foot changes from  $\rho_{vol.} = 0.93$  and  $0.99$  (CO.) to  $0.91$  and  $0.96$  (CTR.). Such a difference of the  $n_e$  profile changes the position where the pressure gradient and the bootstrap current become maximum as shown in Figs.1 (b) and (d).

The MHD stability with a toroidal rotation is investigated with the MINERVA stability code [12] and the initial value code solving the ballooning equation with toroidal flow [13]. The MINERVA code solves the Frieman-Rosenbluth (F-R) equation [14]

$$\rho \frac{\partial^2 \xi}{\partial t^2} + 2\rho(\mathbf{u} \cdot \nabla) \frac{\partial \xi}{\partial t} + \rho(\mathbf{u} \cdot \nabla)(\mathbf{u} \cdot \nabla)\xi = F(\xi), \quad (1)$$

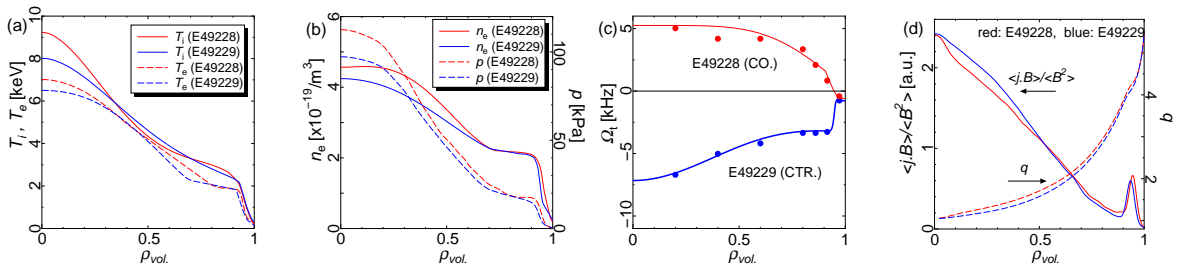


FIG. 1. Profiles of (a)  $T_i$  and  $T_e$ , (b)  $n_e$  and  $p$ , (c)  $\Omega_t$ , (d)  $\langle \mathbf{j} \cdot \mathbf{B} \rangle / \langle B^2 \rangle$  and  $q$ , in the E49228 (CO.) and the E49229 (CTR.) plasmas, respectively.

as the initial value problem. Here  $\rho$  is the plasma mass density,  $\mathbf{u}$  is the equilibrium rotation velocity,  $\mathbf{F}$  is the force operator, and  $\boldsymbol{\xi}$  is the displacement vector. In case that a plasma rotates only in a toroidal direction,  $\mathbf{u}$  can be written as  $\mathbf{u} = \Omega \mathbf{e}_\phi$ , where  $\phi$  is a toroidal angle. Since the MINERVA code is developed with the flux coordinate system, the plasma surface is determined by cutting off the flux surface at  $\psi = 0.995$  when an equilibrium has a separatrix at the last closed flux surface. In this section, the range of  $n$  of the analyzed MHD modes is from 1 to 30, and  $\infty$ , and the shape of the conducting wall surrounding the plasma is approximately the same as that of JT-60U vacuum vessel.

Figure 2 shows the stability diagrams on the  $(\langle j_{ped} \rangle / \langle j \rangle, \alpha_{94})$  plane in (a) the CO. and (b) the CTR. plasmas, where  $j_{ped}$  is the current density averaged over  $(2\psi_{ped} - 1.0) \leq \psi \leq 1.0$ ,  $\alpha$  is the normalized pressure gradient defined as  $\alpha \equiv -(\mu_0/2\pi^2)(dp_0/d\psi)(dV/d\psi)(VR/2\pi)^{0.5}$ ,  $\mu_0$  is the permeability in the vacuum, and the subscript 94 expresses the value at  $\psi = 0.94$ . The target expresses the equilibrium values observed experimentally, and the solid and the broken lines show the stability boundary with and without a toroidal rotation effect, respectively. As shown in Fig.2 (a), the CO. plasma is approximately on the stability boundary of the edge localized MHD mode without a toroidal rotation effect. In fact, the  $n = 12$  peeling-ballooning mode becomes marginally unstable by increasing  $\alpha_{94}$  about 10%; this increment is thought to be within the error of the edge profile measurements. Moreover, the stability boundary changes little even when the toroidal rotation is taken into account in the MHD stability analysis.

On the other hand, as shown in Fig.2 (b), the CTR. plasma is far from the stability boundary without a toroidal rotation, and to make the plasma unstable, it is necessary to increase  $\alpha_{94}$  more than 25%. Since such a large increment in pressure is no longer within the margin of the error, this CTR. plasma without a toroidal rotation is stable against ideal MHD modes. In this CTR. plasma, however, the toroidal rotation moves the stability boundary to the smaller  $\alpha_{94}$  side, and as the result, the maximum pressure gradient becomes smaller from  $\alpha_{94-max} \simeq 2.87$  to  $\simeq 2.28$  under the same  $\langle j_{ped} \rangle / \langle j \rangle \simeq 0.5$  condition. Moreover, the  $n$  number of the MHD modes, which determines the stability boundary, becomes larger as the rotation frequency increases, and the destabilizing effect of the toroidal rotation becomes stronger as the  $n$  number of the MHD mode increases. For example, on the stability boundary at  $\langle j_{ped} \rangle / \langle j \rangle \simeq 0.5$ , the  $n$  number of the MHD mode changes from 16 to 20 by the toroidal rotation. This result is consistent with the results of the qualitative and quantitative analyses about the effects of a rotation and its shear on the edge MHD stability in Refs. [7, 12, 15], and resolves the discrepancy that the edge localized MHD mode is stable in the CTR. ELMy H-mode plasma without the toroidal rotation [16].

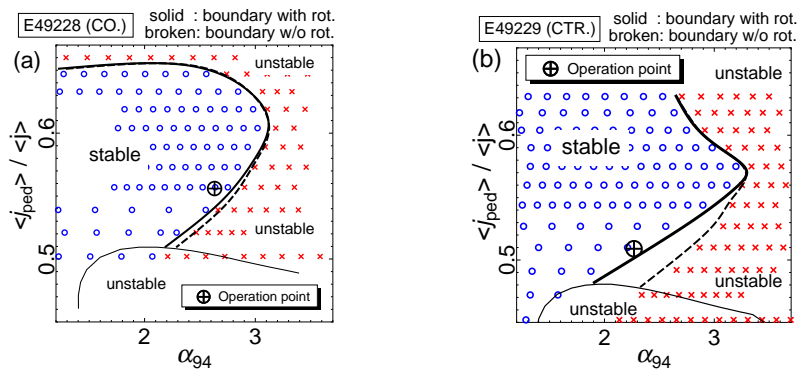


FIG. 2. Stability diagrams on the  $(\langle j_{ped} \rangle / \langle j \rangle, \alpha_{94})$  plane in (a) the CO. (E49228) and (b) the CTR. (E49229) plasmas, respectively. The target expresses the equilibrium values observed experimentally, the (blue) circle means stable with a toroidal rotation, (red) cross means unstable without a toroidal rotation, and the solid and the broken lines show the stability boundary of the finite- $n$  MHD modes and the infinite- $n$  ballooning with and without a toroidal rotation, respectively.

### 3. Mechanisms of a plasma rotation effect on the edge MHD stability

In this section, we investigate mechanisms that a toroidal rotation with shear destabilizes an edge localized MHD mode. Note that as mentioned in Ref. [12], an equilibrium pressure is no longer a flux function when a plasma rotates, and under the isothermal condition on each magnetic surface, an equilibrium pressure can be written as

$$p = p_0(\psi) \exp \left[ M^2 \left( \frac{R^2}{R_0^2} - 1 \right) \right]. \quad (2)$$

Here  $R$  is the coordinate in the  $(R, Z, \phi)$  system, and  $M$  is the Mach number. The equilibrium in this section has a up-down symmetric D-shape cross-section; the ellipticity  $\kappa$  and the triangularity  $\delta$  are (1.74, 0.48) as shown in Fig.3 (a). The parameters ( $R_0$ [m],  $a_0$ [m],  $B_0$ [T],  $I_p$ [MA],  $\beta_p$ ) are (3.00, 0.97, 2.50, 3.00, 1.00), and the profiles of  $dp_0/d\psi$ ,  $\langle \mathbf{j} \cdot \mathbf{B} \rangle / \langle B^2 \rangle$ , and  $\Omega_t$  are given as

$$\frac{dp_0(\psi)}{d\psi} = \beta_p \left( (1 - \psi^5)^{1.5} + 3.5 \cdot \exp \left( -\frac{(\psi - 0.96)^2}{2.25 \times 10^{-4}} \right) \right), \quad (3)$$

$$\frac{\langle \mathbf{j} \cdot \mathbf{B} \rangle}{\langle B^2 \rangle} \propto (1 - \psi^{1.5})^{1.2} + 0.75 \cdot \exp \left( -\frac{(\psi - 0.96)^2}{4 \times 10^{-4}} \right), \quad (4)$$

$$\Omega_t(\psi)[\text{krad/s}] = (50.0 - 0.5)(1.00 - \psi^{48})^4 + 0.5, \quad (5)$$

where  $R_0$  and  $a_0$  are the major and the minor radii of the plasma. Figure 3 shows the profiles of (b)  $p_0$  in Eq.(2) and  $dp_0/d\psi$ , (c)  $\langle \mathbf{j} \cdot \mathbf{B} \rangle / \langle B^2 \rangle$  and  $q$ , and (d)  $\Omega_t/\omega_{A0}$  and  $M$  of the equilibrium, where  $\omega_{A0}$  is the toroidal Alfvén frequency at axis. The second term in the right hand side (RHS) of Eq.(3) and that of Eq.(4) make the steep pressure gradient and the virtual edge bootstrap current density near  $\psi = 0.96$ , respectively. The range of  $n$  of the MHD mode analyzed numerically is from 1 to 50, and the conducting wall is placed at  $d/a = 2.00$ .

Figure 4 shows the  $n$  dependences of the growth rate  $\gamma$  and the mode frequency divided by  $n$ ,  $\omega$ , with and without the sheared toroidal rotation. From this figure, we can follow that the  $n$  number of the unstable MHD mode is between 11 and 29 in the static case. However, the sheared toroidal rotation destabilizes the MHD modes, and as the result, the  $n = 9, 10$  and  $30 \leq n \leq 36$  modes become unstable.

Based on this numerical result, we try to clarify destabilizing mechanisms by using the F-R equation Eq.(1) with the assumption that the displacement  $\xi$  is the eigenmode with the complex eigenvalue  $\lambda$ . By multiplying  $\xi$  on the left side of Eq.(1) and executing a volume integral in the system with the assumption  $\xi(\mathbf{x}, t) \equiv \bar{\xi}(\mathbf{x}) \exp(\lambda t)$ , we can obtain the following equation

$$\begin{aligned} & \lambda^2 \langle \bar{\xi} | \rho | \bar{\xi} \rangle + 2\lambda \langle \bar{\xi} | \rho (\mathbf{u} \cdot \nabla) | \bar{\xi} \rangle \\ & + \langle \bar{\xi} | \rho (\mathbf{u} \cdot \nabla) (\mathbf{u} \cdot \nabla) | \bar{\xi} \rangle = \langle \bar{\xi} | \mathbf{F}(\bar{\xi}) \rangle, \end{aligned} \quad (6)$$

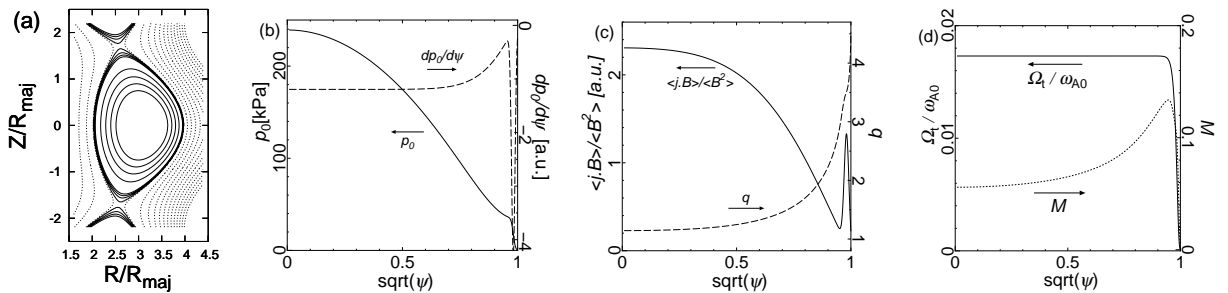


FIG. 3. (a) Contours of the poloidal magnetic flux  $\psi$  (magnetic surfaces) of the equilibrium. Profiles of (b)  $p_0$  and  $dp_0/d\psi$ , (c)  $\langle \mathbf{j} \cdot \mathbf{B} \rangle / \langle B^2 \rangle$  and  $q$ , and (d)  $\Omega_t/\omega_{A0}$  and  $M$ .

where  $\langle \bar{\xi} | \Pi | \bar{\xi} \rangle \equiv \int_{V_{tot}} \bar{\xi}^* \cdot \Pi \cdot \bar{\xi} d\tau$ , and  $d\tau$  is the volume element. In case that the eigenvector  $\bar{\xi}$  is already known,  $\lambda = \gamma + in\omega$  can be calculated with the quadratic formula of Eq.(6) as

$$\lambda = \frac{-\delta W_c \pm \sqrt{\delta W_c^2 - \delta K \cdot \delta W_p}}{\delta K}. \quad (7)$$

Here  $\delta K$ ,  $\delta W_c$ , and  $\delta W_p$  are defined as

$$\delta K = \langle \bar{\xi} | \rho | \bar{\xi} \rangle, \quad (8)$$

$$\delta W_c = \langle \bar{\xi} | \rho(\mathbf{u} \cdot \nabla) | \bar{\xi} \rangle, \quad (9)$$

$$\delta W_p = \langle \bar{\xi} | \rho(\mathbf{u} \cdot \nabla)(\mathbf{u} \cdot \nabla) | \bar{\xi} \rangle - \langle \bar{\xi} | \mathbf{F}(\bar{\xi}) \rangle. \quad (10)$$

Hereafter, the subscript of  $\bar{\xi}$  is omitted. As is well-known, since the operators  $\rho$  and  $\rho(\mathbf{u} \cdot \nabla)(\mathbf{u} \cdot \nabla) - \mathbf{F}$  are Hermitian, and  $\rho(\mathbf{u} \cdot \nabla)$  is anti-Hermitian,  $\delta K$ ,  $\delta W_p$  are real, and  $\delta W_c$  is imaginary, respectively. With these properties, when a MHD mode is unstable, the growth rate  $\gamma$  and the mode frequency  $\omega$  can be written as

$$\gamma = \pm \frac{\sqrt{\delta W_c^2 - \delta K \cdot \delta W_p}}{\delta K}, \quad (11)$$

$$in\omega = -\frac{\delta W_c}{\delta K}. \quad (12)$$

To discuss the MHD stability in analogy with the Energy Principle in the static plasma, we define the new energy  $\delta W_g$  as

$$\gamma^2 \delta K^2 = \delta W_c^2 - \delta K \cdot \delta W_p \equiv -\delta K \delta W_g. \quad (13)$$

This  $\delta W_g$  expresses whether the plasma is stable or unstable by its sign, and becomes the same as the potential energy in the static plasma.

Next, we separate  $\delta W_g$  into two terms. One is the term that expresses the potential energy taking into account the change of the equilibrium by the rotation  $((\mathbf{u} \cdot \nabla)\mathbf{u})$ ,  $\delta W_{g-eq.}$ , and the other expresses the rotation effect on the displacement explicitly through the component  $(\mathbf{u} \cdot \nabla)\xi$ ,  $\delta W_{g-rot.}$ ; these can be written as

$$\delta W_g = \delta W_{g-eq.} + \delta W_{g-rot.}, \quad (14)$$

$$\delta W_{g-eq.} = -\langle \xi | \mathbf{F}(\xi) \rangle, \quad (15)$$

$$\delta W_{g-rot.} = \langle \xi | \rho(\mathbf{u} \cdot \nabla)(\mathbf{u} \cdot \nabla) | \xi \rangle - \frac{\langle \xi | \rho(\mathbf{u} \cdot \nabla) | \xi \rangle^2}{\delta K}. \quad (16)$$

The first term in RHS of Eq.(16) represents approximately the Doppler shift due the plasma rotation, and the second term in RHS of Eq.(16) can be written as

$$-\frac{\langle \xi | \rho(\mathbf{u} \cdot \nabla) | \xi \rangle^2}{\delta K} = n^2 \omega^2 \delta K = n^2 \omega^2 \langle \xi | \rho | \xi \rangle, \quad (17)$$

This means that  $\delta W_{g-rot.}$  expresses the energy induced by the difference between the eigenmode frequency and the toroidal rotation frequency of the plasma. With these energies defined here, we discuss mechanisms that an edge localized MHD mode becomes unstable by a toroidal rotation with shear.

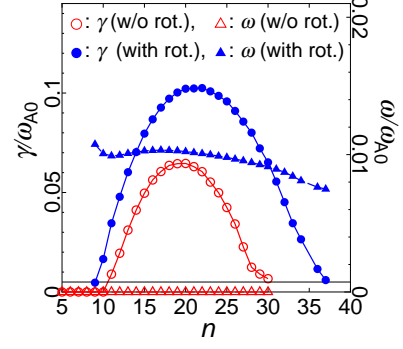


FIG. 4. Dependences on  $n$  of  $\gamma$  and  $\omega$  with and without the sheared toroidal rotation.

Figure 5 shows the  $n$  dependences of  $\delta W_g$ ,  $\delta W_{g-eq.}$ , and  $\delta W_{g-rot.}$  of the peeling-ballooning mode, whose stability is already investigated as shown in Fig.4; that of  $\delta W_g$  in the static case is also plotted. As shown in this figure,  $\delta W_{g-rot.}$  becomes negative by the sheared toroidal rotation and plays an important role for destabilizing the MHD modes even though  $\delta W_{g-eq.}$  is positive. This result indicates that the mechanism that a toroidal rotation with shear destabilizes an edge localized MHD mode is the difference between the eigenmode frequency and the toroidal rotation frequency of the plasma. It is noted that there is a trend that the destabilizing effect from  $\delta W_{g-rot.}$  becomes larger as  $n$  increases. This trend is consistent with the results in the previous section and the past works [6, 7], and is mainly come from the leading order term in the  $n$  expansion of  $\delta W_{g-rot.}$  and the mode structure of  $\xi$  [15].

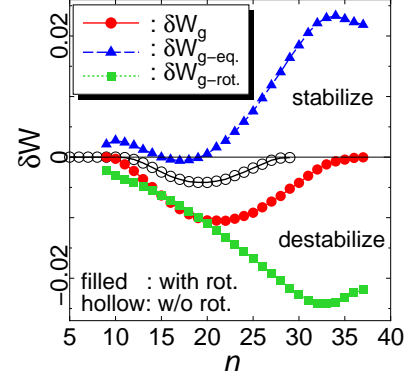


FIG. 5. Dependences on  $n$  of  $\delta W_g$ ,  $\delta W_{g-eq.}$  and  $\delta W_{g-rot.}$  for the peeling-ballooning mode stability.

#### 4. Effects of a poloidal rotation on the edge MHD stability

As identified in the previous section, the destabilizing effect depends on the mode frequency  $\omega$ . Since the mode frequency can be evaluated with Eq.(12), the operator  $(\mathbf{u} \cdot \nabla)$  is essential for determining  $\omega$ . If we can assume that a centrifugal force and a Coriolis force are negligible,  $(\mathbf{u} \cdot \nabla)$  is identical to  $\mathbf{k} \cdot \mathbf{u}$ , where  $\mathbf{k}$  is the wave number vector. In the case that a plasma rotates in not only a toroidal but also a poloidal directions,  $\mathbf{k} \cdot \mathbf{u}$  becomes  $i(m\Omega_\theta - n\Omega_\phi)$ , where  $m$  is the poloidal mode number,  $\Omega_\theta$  and  $\Omega_\phi$  are the plasma rotation frequency in the poloidal and the toroidal directions. As mentioned in Introduction, a poloidal rotation is no longer negligible at edge pedestal. Furthermore, the  $m$  number in  $\mathbf{k} \cdot \mathbf{u}$  is about  $q$  times larger than the  $n$  number, because each poloidal Fourier component of an ELM usually localizes near each rational surface  $\mathbf{k} \cdot \mathbf{B} = m - nq = 0$ . These imply that a poloidal rotation also can affect the edge MHD stability by changing the mode frequency. In this section, we investigate this effect numerically.

In general,  $\Omega_\theta$  and  $\Omega_\phi$  are not flux functions  $f(\psi)$ . On the other hand, in toroidally rotating plasmas, a toroidal rotation frequency can be regarded as a flux function  $\Omega_t(\psi)$ . To compare the result in the plasma that rotates both toroidally and poloidally with that in the pure toroidally rotating plasma, we determine the rotation profile as follows. At first, we investigate the MHD stability in the pure toroidally rotating plasma with  $\mathbf{u} = \Omega_t \mathbf{e}_\phi$ . After that,  $\Omega_\phi(\psi, Z = 0)$  is adjusted as  $\Omega_t$ , and  $\Omega_\theta(\psi, Z = 0)$  is determined arbitrary. As discussed in Ref. [17], due to the conservation law of momentum, an equilibrium rotation can be expressed as

$$\mathbf{u} = \frac{\Phi(\psi)}{\rho} \mathbf{B} + \Omega_t(\psi) \mathbf{e}_\phi, \quad (18)$$

where  $\Phi$  is a surface value related to a momentum in the direction parallel to the magnetic field. In Eq.(18), a poloidal component is only in the first term in RHS, the plasma rotation profile can be determined as

$$\frac{\Phi(\psi)}{\rho} = \frac{qR}{B_t} \Omega_\theta(\psi, Z = 0), \quad (19)$$

$$\Omega_t(\psi) = \Omega_\phi(\psi, Z = 0) - q\Omega_\theta(\psi, Z = 0). \quad (20)$$

Here  $\theta$  is defined as the straight field line coordinate used in MINERVA [12]. Based on this rule, an effect of a poloidal rotation on edge MHD stability is investigated with the equilibria shown in Fig.3;  $\Omega_\phi(\psi, Z = 0)$  is equal to  $\Omega_t$  in Eq.(5), and  $\Omega_\theta(\psi, Z = 0)$  is determined later.

Note that many previous works showed that a poloidal rotation can change an equilibrium drastically from that without a rotation [18]; in particular, a transonic poloidal rotation can give rise to shock waves. However, a poloidal rotation in tokamak plasmas is not likely so large. In addition, as mentioned above, we pay attention to the effect of a poloidal rotation on the MHD stability due to the change of the mode frequency. From this viewpoint, in this paper, an effect of a poloidal rotation on an equilibrium is assumed as negligible, and that on the linear equation of motion Eq.(1) is to be investigated.

Figure 6 (a) shows profiles of  $\Omega_\phi$  and  $\Omega_\theta$  at  $Z = 0$  near pedestal. The profiles of the positive  $\Omega_\theta$  and the negative one are determined to make  $\Omega_t(\psi) = 0.5\Omega_\phi(\psi, Z = 0)$  and  $\Omega_t(\psi) = 1.5\Omega_\phi(\psi, Z = 0)$ , respectively. In the positive  $\Omega_\theta$  case shown in Fig.6 (b), which shows the  $n$  dependences of  $\gamma$  and  $\omega$ , the mode frequency becomes about half by adding the poloidal rotation. The reason of this frequency decay is attributed to the decrease of  $\mathbf{k} \cdot \mathbf{u}$  near the rational surfaces as mentioned previously. However, even though the mode frequency becomes about half, the poloidal rotation has little impact on the stability of the MHD modes whose  $n \leq 20$ . For  $n > 20$  modes, this makes the growth rates smaller than those in the pure toroidally rotating case, but the difference of  $\gamma$  is not so large that it is expected from the decrease of  $\delta W_{g-rot.}$  due to the frequency decay.

Meanwhile, when the sign of the poloidal rotation frequency is negative, the poloidal rotation can change the edge MHD stability. In this case, Figure 6 (c) indicates that  $\omega$  becomes about 1.5 times larger than that in the pure toroidally rotating case. This result can be explained in the same way when  $\Omega_\theta$  is positive. However, unlike in the previous case,  $\gamma$  of  $n > 20$  modes becomes larger; for example, the maximum  $\gamma$  value becomes about 1.4 times larger than that without  $\Omega_\theta$ . In this case, the increase of  $\delta W_{g-rot.}$  is responsible for the destabilization.

The results in this section show that a poloidal rotation can change the edge MHD stability due to changing the mode frequency, and this effect depends on not only the absolute value but also the sign of the frequency when the plasma also rotates in the toroidal direction.

## 5. Summary

An effect of a toroidal rotation with shear on a type-I ELM stability has been investigated numerically in JT-60U ELMy H-mode plasmas. As the result of the stability analysis, we have clarified that the toroidal rotation observed experimentally can destabilize edge localized MHD modes, and can make the stability boundary of edge localized MHD modes close to the point of equilibrium observed experimentally in the stability diagram, though this point is far from the

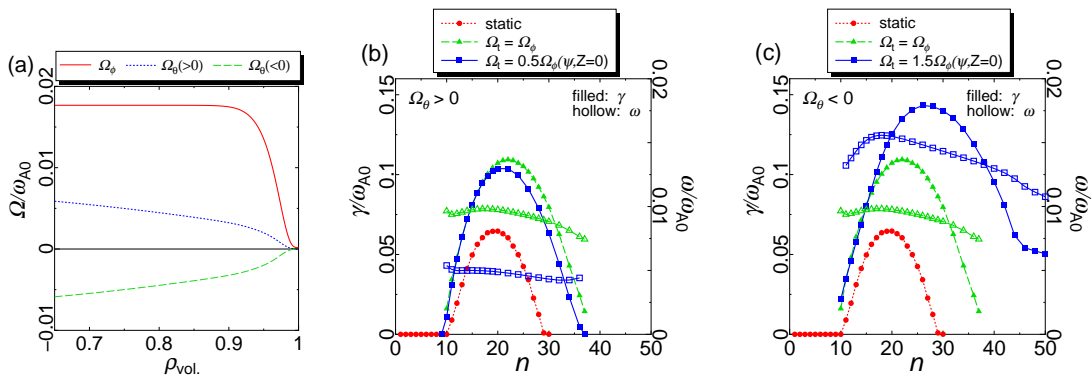


FIG. 6. (a) Profiles of  $\Omega_\phi$  and  $\Omega_\theta$  at  $Z = 0$  near pedestal. The  $\Omega_\theta$  profiles are determined to make  $\Omega_t(\psi) = 0.5\Omega_\phi(\psi, Z = 0)$  when  $\Omega_\theta > 0$  and  $\Omega_t(\psi) = 1.5\Omega_\phi(\psi, Z = 0)$  when  $\Omega_\theta < 0$ , respectively. (b), (c) Dependences on  $n$  of  $\gamma$  and  $\omega$  in the static, the pure toroidally rotating and both toroidally and poloidally rotating cases; ((b) positive  $\Omega_\theta$ , (c) negative  $\Omega_\theta$ ).

stability boundary under the static assumption.

To identify a mechanism of this destabilization, we have introduced new definitions of energy that are distinguished by physics. By comparing these energies, we have clarified that this destabilization by a toroidal rotation with shear is mainly induced by the difference between the eigenmode frequency and the toroidal rotation frequency of the plasma, and this effect tends to be larger as the toroidal mode number of the MHD mode increases.

Based on the result that the destabilizing effect depends on the mode frequency, we have paid attention to effects of not only a toroidal rotation but also a poloidal rotation on the edge MHD stability. When a poloidal rotation is added in a toroidally rotating plasma, the mode frequency drastically changes because a rotation parallel to the magnetic field has little impact on the mode frequency. By determining the direction of a poloidal rotation to increase a mode frequency, the edge localized MHD mode becomes more unstable. However, when a plasma rotates poloidally in the opposite direction, the growth rate of edge localized MHD modes decreases. These results indicate that a poloidal rotation can change the edge MHD stability due to changing the mode frequency, and this effect depends on not only the absolute value but also the sign of the frequency when the plasma also rotates in the toroidal direction.

### Acknowledgments

We would like to thank Dr. M. Mori and Dr. T. Ozeki for their continuous encouragement support. This work was partially supported by the Ministry of Education, Science, Sports and Culture, Grant-in-Aid for Young Scientists (B), 2009, 21760698.

### References

- [1] Doyle E J et al. 2007 *Nucl. Fusion* **47** S18
- [2] Oyama N et al. 2007 *Plasma Phys. Control. Fusion* **49** 249
- [3] Urano H et al. 2007 *Nucl. Fusion* **47** 706
- [4] Oyama N et al. 2005 *Nucl. Fusion* **45** 871
- [5] Oyama N et al. 2010 *Nucl. Fusion* **50** 064014
- [6] Snyder P B et al. 2007 *Nucl. Fusion* **47** 961
- [7] Aiba N, Tokuda S, Furukawa M, Oyama N and Ozeki T 2009 *Nucl. Fusion* **49** 065015
- [8] Stacey W M and Groebner R J 2008 *Phys. Plasmas* **15** 012503
- [9] Kamiya K et al. 2010 *Phys. Rev. Lett.* **105** 045004
- [10] Kojima A et al. 2009 *Nucl. Fusion* **49** 115008
- [11] Tani K, Azumi M and Devoto R S J 1992 *J. Comput. Phys.* **98** 332
- [12] Aiba N et al. 2009 *Comput. Phys. Commun.* **180** 1282
- [13] Furukawa M, Tokuda S and Wakatani M 2003 *Nucl. Fusion* **43** 425
- [14] Frieman E and Rotenberg M 1960 *Rev. Mod. Phys.* **32** 898
- [15] Aiba N, Furukawa M, Hirota M, Tokuda S 2010 *Nucl. Fusion* **50** 045002
- [16] Aiba N, Oyama N, Kojima A and Tokuda S 2010 *J. Plasma Fusion Res. Ser.* **9** 74
- [17] Tokuda S 1998 *J. Plasma Fusion Res.* **74** 503
- [18] Grad H 1960 *Rev. Mod. Phys.* **32** 830